

Induction of Molecular Chirality by Circularly Polarized Light in Cyclic Azobenzene with a Photoswitchable Benzene Rotor

P. K. Hashim, Reji Thomas, and Nobuyuki Tamaoki*^[a]

Abstract: New phototriggered molecular machines based on cyclic azobenzene were synthesized in which a 2,5-dimethoxy, 2,5-dimethyl, 2,5-difluorine or unsubstituted-1,4-dioxybenzene rotating unit and a photoisomerizable 3,3'-dioxyazobenzene moiety are bridged together by fixed bismethylene spacers. Depending upon substitution on the benzene moiety and on the *E/Z* conformation of the azobenzene unit, these molecules suffer various degrees of restriction on the free rotation of the benzene rotor. The rotation of the substituted benzene rotor within the cyclic azobenzene cavity imparts planar chirality to the molecules. Cyclic azobenzene **1**, with methoxy groups at both the 2- and 5-positions of the benzene rotor, was so conformationally re-

stricted that free rotation of the rotor was prevented in both the *E* and *Z* isomers and the respective planar chiral enantiomers were resolved. In contrast, compound **2**, with 2,5-dimethylbenzene as the rotor, demonstrated the property of a light-controlled molecular brake, whereby rotation of the 2,5-dimethylbenzene moiety is completely stopped in the *E* isomer (brake ON, rotation OFF), while the rotation is allowed in the *Z* isomer (brake OFF, rotation ON). The cyclic azobenzene **3**, with fluorine substitution on the benzene rotor, was in the brake OFF state re-

gardless of *E/Z* photoisomerization of the azobenzene moiety. More interestingly, for the first time, we demonstrated the induction of molecular chirality in a simple monocyclic azobenzene by circular-polarized light. The key characteristics of cyclic azobenzene **2**, that is, stability of the chiral structure in the *E* isomer, fast racemization in the *Z* isomer, and the circular dichroism of enantiomers of both *E* and *Z* isomers, resulted in a simple reversible enantio-differentiating photoisomerization directly between the *E* enantiomers. Upon exposure to *r*- or *l*-circularly polarized light at 488 nm, partial enrichment of the (*S*)- or (*R*)-enantiomers of **2** was observed.

Keywords: azo compounds • chirality • circular dichroism • molecular devices • photochromism

Introduction

Induction of chirality in molecules or molecular assemblies has attracted the interest of chemists for a long time, particularly in connection with homochiral structures in nature.^[1–5] In addition to the academic interest, the induction of chirality is also important in modern chemistry due to the increased number of applications in material science^[6] and technology.^[7,8] Several physical factors were found to contribute to the enantiomeric imbalance in a racemic system. The various physical factors so far used to achieve such enrichment include mechanical stirring^[9] and the introduction of a chiral environment in the form of chiral solvents^[10] or chiral additives.^[11] In this context, the chiral nature of light has also been used for chiral induction; indeed, the chirality of light is believed to be one of the origins of homochiral structures observed in nature.^[1,12] Moreover, the intriguing

science behind photoinduced chirality is also attracting the attention of many researchers owing to its the possible applications in chiral sensors^[13] and switches.^[14]

Following studies by le Bel^[15] and Van't Hoff^[16] that demonstrated the potential usefulness of *l*- or *r*-circular polarized light (*l*- or *r*-CPL), several attempts have been made to achieve enantiomeric enrichment using CPL. Among the various photocontrolled chiral induction processes, reversible enantio-differentiating photoisomerization is known to take place in a number of compounds for which photoresolution and photoracemization occur with CPL and normal light, respectively.^[17–19] In 1996, Feringa and co-workers reported^[8b,18] dynamic photoresolution mediated by CPL irradiation on a sterically overcrowded alkene system, but the process required relatively long irradiation time and the enantiomeric excess was less than anticipated. Azobenzene is another notable class of photochromic molecule with remarkable *E/Z* isomerization that has been widely used for the sophisticated fabrication and development of molecular machines,^[20] molecular conductors,^[21] optical memory devices,^[22] and optical switches.^[23,14e–g] In addition, there are several reports in the literature on azobenzene-based polymers and liquid crystals for which the chiral molecular order is introduced by CPL irradiation.^[24] In our previous report we described the partial photoresolution of a bicyclic azoben-

[a] P. K. Hashim, Dr. R. Thomas, Prof. N. Tamaoki
Research Institute for Electronic Science
Hokkaido University, N20, W10
Sapporo, Hokkaido 001-0020 (Japan)
Fax: (+81) 11-706-9357
E-mail: tamaoki@es.hokudai.ac.jp

Supporting information for this article is available on the WWW under <http://dx.doi.org/10.1002/chem.201003526>.

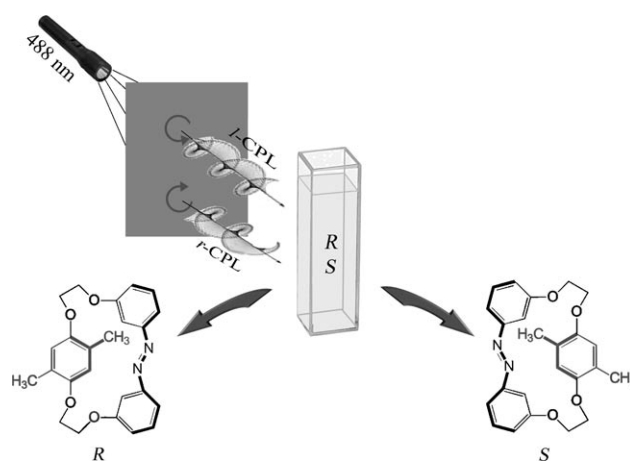
zene dimer with a relatively large difference in the molar extinction coefficient between enantiomers.^[25] However, this bicyclic system, with two photoresponsive components, resulted in a complicated enantio-differentiating photoisomerization path with three isomers (*EE*, *EZ* and *ZZ*), which made the precise estimation of actual enantiomeric enrichment upon CPL irradiation difficult. To the best of our knowledge, no further examples of efficient systems exhibiting sufficient photoresolution within short irradiation times have been reported in the literature.

Our group is particularly interested in the design and synthesis of azobenzene molecular systems to explore various applications such as chiral dopants in liquid crystals and photodriven brake systems.^[14,26] Recently, we reported the synthesis of a planar chiral azobenzene consisting of a dioxynaphthalene moiety that was cyclically bonded at the *meta* positions of azobenzene by bismethylene spacers, which was successfully employed as a chiroptical switch in commercially available liquid crystals, giving rise to photo-tunable reflection colors.^[14a] More recently, in a similar design, by tuning the spacer lengths we demonstrated for the first time a complete ON/OFF switching of a naphthalene rotor by *E/Z* photoisomerization of an azobenzene braking element.^[26]

In the present work we demonstrate a new class of cyclic azobenzene with a substituted benzene rotor showing a photoswitchable braking property. We studied the effect of steric bulk of the substituents at the 2- and 5-positions of the benzene ring on the rotational behavior of the rotor in a fixed cyclic azobenzene cavity. Similar to our previous naphthalene-based cyclic azobenzene, the compound with a 2,5-dimethyl benzene rotor showed enantiomer stability in the *E* isomer and fast racemization in the *Z* isomer. In addition, this molecule exhibited a reasonably high $\Delta\epsilon$ value, which allowed it to be used in a chiral induction study with CPL. The compound with a 2,5-dimethyl benzene rotor exhibits a simple reversible enantio-differentiating photoisomerization path between the *E* enantiomers, along with a considerable induced circular dichroism (ICD) within a short period of CPL irradiation (Scheme 1). To best of our knowledge, this is the first monocyclic azobenzene that shows an enantiomeric excess that is induced by CPL irradiation.

Results and Discussion

Synthesis and conformational analysis: In the present study, we designed and synthesized a new series of cyclic azobenzenes (**1–4**) consisting of either an unsubstituted or a 2,5-disubstituted (methoxy, methyl, or fluorine) 1,4-dioxybenzene rotating unit, and a 3,3'-dioxyazobenzene photoisomerizable moiety, bridged together by fixed bismethylene spacers. The incorporation of a 2,5-disubstituted 1,4-dioxybenzene ring system can impart an element of planar chirality to the molecule, provided there is no free rotation of the benzene unit through the cavity of macrocycle.^[25] Although the difference in the electronic properties of the substituents (methoxy,

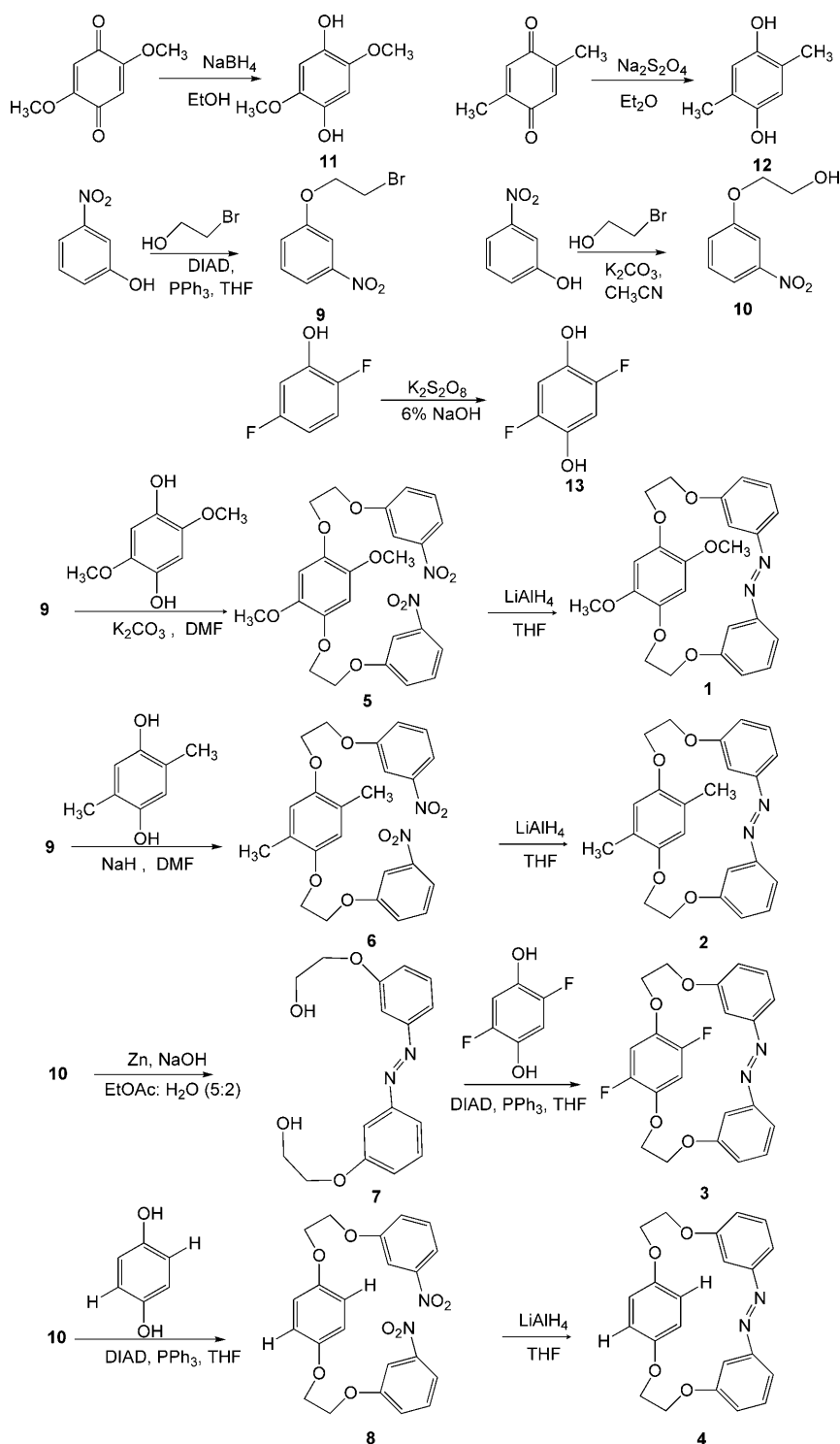


Scheme 1. Schematic illustration of chirality induction by CPL. This study did not address which of the enantiomers *R* or *S* was enriched by *l*- or *r*-CPL irradiation.

methyl or fluorine) can affect the rotation, we considered this to be negligible, and expected steric factors to determine the rotational speed of the substituted benzene rotors. That is, the size of the substituent, as well as control of the volume of the cavity by photoisomerization, can be the deciding factors for rotor movement.

The synthetic strategies used to obtain the target molecules are shown in Scheme 2. Compounds **1**, **2**, and **4** were synthesized in three steps through reduction of the corresponding dinitro compounds under dilute conditions. However, in the case of compound **3**, with difluoro benzene as rotor, an extremely low yield of the corresponding dinitro compound was observed. Therefore, we adopted another route in which the cyclization was carried out by conducting a Mitsunobu reaction under dilute conditions (see Experimental Section).

Figure 1 shows the ¹H NMR spectra of (*E*)-**1**, (*E*)-**2**, and (*E*)-**3** recorded at room temperature. The spectrum of (*E*)-**1** displayed a doublet of triplets at $\delta=4.63$ – 4.58 ppm (2H) and multiplet resonances including a hidden doublet of triplets at $\delta=4.52$ – 4.37 ppm (6H) for the bismethylene protons [-OCH^aH^bCH₂O-]. ¹H NMR spectra of (*E*)-**2**, with methyl substituents on the benzene ring, clearly displayed two sets of separated doublet of triplets at $\delta=4.64$ and 4.31 ppm (2H each, -OCH^aH^bCH₂O-) and another resonance at $\delta=4.42$ ppm due to aliphatic methylene protons. The split resonances for H^a and H^b can be explained by a halted rotation of the benzene unit, which results in a different environment for these diastereotopic protons. This result provided a preliminary insight into the degree of rotation of the benzene moiety through the cyclic azobenzene cavity for (*E*)-**1** and (*E*)-**2**, which imparts planar chirality to the molecule. NOESY experiments (see Figure S3 in the Supporting Information) indicated that the protons at $\delta=4.52$ – 4.37 ppm for (*E*)-**1** and at $\delta=4.64$ ppm for (*E*)-**2** are close to these aromatic protons (i.e., far from the methyl or methoxy substituents) of the 2,5-disubstituted benzene rotor. In contrast, the ¹H NMR spectra for (*E*)-**3**, with fluorine substituents at the



Scheme 2. Synthetic route to the molecules 1–4.

2,5-positions of the benzene rotor, displayed two triplets without splitting at $\delta = 4.51$ and 4.42 ppm for aliphatic protons (Figure 1), clearly indicating the allowed rotation of the 2,5-difluorobenzene rotor through the macrocyclic cavity in the *E* isomer. In the case of compound 4, with an unsubstituted benzene rotor, the extent of rotation of the benzene ring through macrocyclic cavity could not be evaluated from

the NMR study, owing to the absence of diastereotopic hydrogen atoms. Presumably, this molecule should also exhibit free rotation of the benzene rotor in the *E* isomer because the hydrogen atom is smaller than the fluorine atom.

Single-crystal X-ray analyses of (*E*)-1 and (*E*)-2 were carried out to confirm the molecular structures (Figure 2). Analysis of crystal structure indicated that, in the *E* isomers, the planes of the azobenzene and benzene rotating units were positioned reasonably close and were in a perpendicular orientation to each other, keeping the methoxy or methyl substituents away from the cavity.

In summary, rotation of the benzene rotor is prevented in compounds 1 and 2 in their *E* form, whereas it is allowed in compounds 3 and 4 on the NMR timescale. This restricted rotation of the disubstituted rotor through the cyclic azobenzene cavity imparts planar chirality to molecules 1 and 2, and would be expected to make the compounds optically resolvable by chiral HPLC. However, optical resolution would not be possible for compound 3 due to the fast rotation of the difluorobenzene rotor.

Photoisomerization of cyclic azobenzenes:

To investigate the photochemical isomerization of the compounds, UV/Vis spectroscopy and HPLC studies were carried out at room temperature. Figure 3 shows the change in the UV/Vis absorption of 2 in ethyl acetate,

on irradiation with light of wavelengths 366 and 436 nm. Upon irradiation at 366 nm, a gradual decrease was seen in the intensity of the $\pi\text{-}\pi^*$ transition band at 327 nm, with a notable increase in the $n\text{-}\pi^*$ transition band at 410–500 nm due to photochemical *E/Z* isomerization. The reverse spectral changes were observed upon irradiation at 436 nm. Similar spectral changes were observed in the case of com-

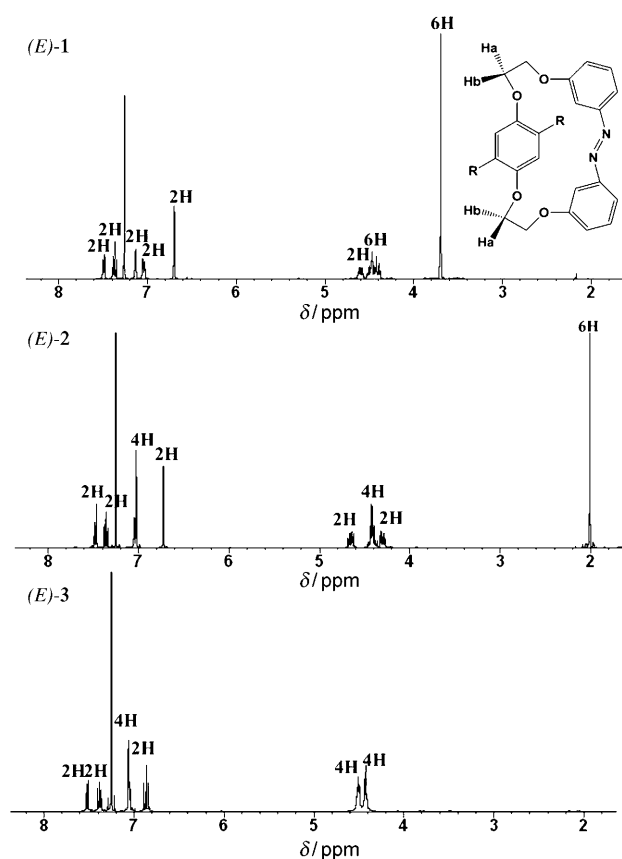


Figure 1. ^1H NMR spectra of cyclic azobenzene (*E*)-1, (*E*)-2, and (*E*)-3 in CDCl_3 at room temperature.

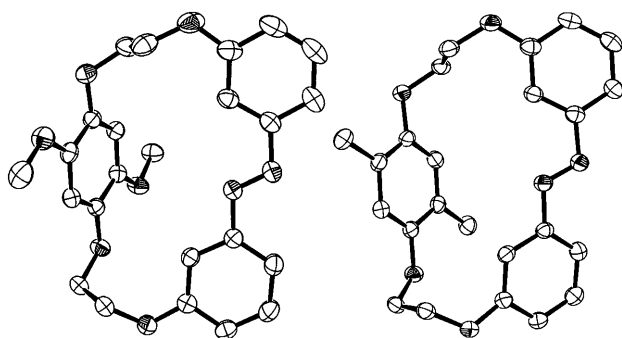


Figure 2. X-ray crystal structures of (*E*)-1 (left) and (*E*)-2 (right).

pounds **1**, **3**, and **4** (see the Supporting Information Figures S4 to S6). The photostationary states ($\text{PSS}_{366\text{ nm}}$ or $\text{PSS}_{436\text{ nm}}$) for compounds **1–4** were attained by irradiating at 366 or 436 nm. The *E* to *Z* isomer compositions at the PSS were estimated by HPLC analysis to be 15:85 and 79:21 for **1**, 11:89 and 75:25 for **2**, and 7:93 and 85:15 for **3**, respectively, at 366 and 436 nm. From the $\text{PSS}_{366\text{ nm}}$, slow thermal back reaction from *Z* to *E* was seen to occur (rate constant $k = 1.94 \times 10^{-6} \text{ s}^{-1}$ at 25.0°C) as observed by the change in the UV/Vis absorption spectra of **2** (see the Supporting Information).

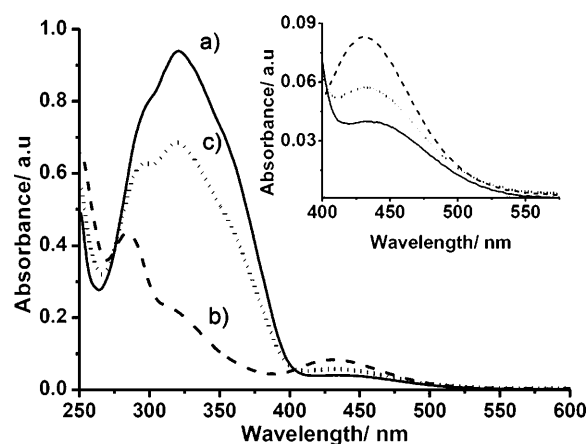


Figure 3. Absorption spectral change of **2** in ethyl acetate upon irradiation at room temperature; a) initial state before irradiation (solid line); b) photostationary state, $\text{PSS}_{366\text{ nm}}$ (dashed line); c) $\text{PSS}_{436\text{ nm}}$ (dotted line). An enlarged view of $n\text{-}\pi^*$ band is shown in the inset.

Effect of the bulkiness of the substituent and photoisomerization on rotor motion: We studied the effect of the bulkiness of the substituent on the rotatory behavior and wanted to introduce a photoswitchable element into the molecular system that would allow complete ON/OFF brake control. A correlation between the bulkiness of the substituent on the benzene rotor and its rotatory behavior was observed in the ^1H NMR study, and was further confirmed by chiral HPLC analyses. The HPLC trace showed two peaks for (*E*)-**1** and (*E*)-**2**, whereas a single peak was seen for (*E*)-**3**. We were even able to separate enantiomers of (*E*)-**1** and (*E*)-**2** on a preparative scale. This observation was in good agreement with the planar chiral nature of (*E*)-**1** and (*E*)-**2**, which originates from the completely stopped rotation of the substituted benzene moiety. To check the possibility of racemization in the *Z* state, HPLC analysis was carried out using a chiral column.

On irradiating racemic (*E*)-**1**, which exhibited two peaks corresponding to (*E*)-**1_A** ($R_t = 22.57$ min) and (*E*)-**1_B** ($R_t = 26.29$ min), at 366 nm, two new peaks assignable to (*Z*)-**1_A** ($R_t = 50.54$ min) and (*Z*)-**1_B** ($R_t = 52.84$ min) were observed; subsequent irradiation at 436 nm resulted in increased intensity of the parent peaks. Starting with pure enantiomer (*E*)-**1_A**, exposure at 366 nm induced the formation of a single new peak ($R_t = 50.54$ min) assignable to (*Z*)-**1_A** and subsequent irradiation at 436 nm resulted in increased intensity of the parent peak without the formation of a peak corresponding to (*E*)-**1_B**. These results confirmed that, even in the *Z* form, racemization does not occur due to rotation of the 2,5-dimethoxybenzene rotor through the macrocyclic cavity (for chromatograms see Figure S8 in the Supporting Information). In contrast, interesting results were observed in the case of **2**, with less bulky methyl groups at the 2-, and 5-positions of the benzene rotor. Racemic (*E*)-**2**, which exhibited two peaks ((*E*)-**2_A** at $R_t = 18.84$ min and (*E*)-**2_B** at $R_t = 22.04$ min) by chiral HPLC, formed a new, single peak ($R_t = 59.03$ min) assignable to (*Z*)-**2** upon irradiation at 366 nm;

this is in sharp contrast to the result obtained with compound **1**, which formed two *Z* isomers (Figure 4a). These results gave a preliminary insight into the fast racemization in

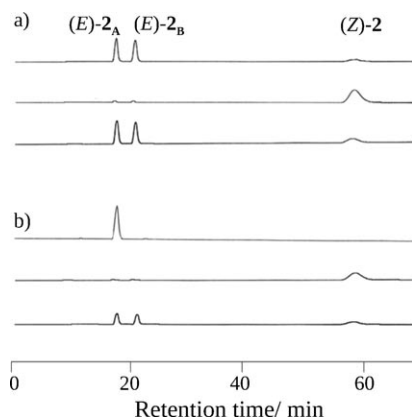


Figure 4. Chromatograms of a) racemic mixture of (*E*)-**2** before irradiation, the PSS after irradiation at 366 nm (PSS_{366 nm}), and the PSS after irradiation at 436 nm (PSS_{436 nm}) (top to bottom), and b) (*E*)-**2**_A before irradiation, the PSS_{366 nm} and the PSS_{436 nm} (top to bottom), obtained by chiral HPLC with a flow rate at 1.5 mL min⁻¹.

the *Z* form of **2**. Subsequent irradiation at 436 nm resulted in increased intensity of the parent peaks. To further confirm the racemization behavior of the *Z* isomer, a separated sample of pure (*E*)-**2**_A was exposed to UV light. The HPLC chromatogram of the irradiated enantiomer (*E*)-**2**_A showed a peak corresponding to (*Z*)-**2**, as observed in the case of racemic **2**. Irradiation of resulting solution at 436 nm induced a reverse isomerization, giving rise to two peaks with the same peak area ($R_t = 18.84$ and 22.04 min) that matched those of the racemized (*E*)-**2**_A and (*E*)-**2**_B (Figure 4b). Thus, the photoinduced *E/Z* isomerization of the separated enantiomers proceeded with racemization, revealing that the macrocyclic cavity for the *Z* isomer is sufficiently large to permit rotation of the 2,5-dimethylbenzene rotor. In contrast, with compounds (*E*)-**1** and (*E*)-**2**, the HPLC chromatogram for (*E*)-**3** showed a single peak ($R_t = 15.24$ min). Compound (*E*)-**3**, upon irradiation at 366 nm, formed a new peak ($R_t = 25.43$ min) assignable to (*Z*)-**3**; visible irradiation (436 nm) resulted in reversal to the *E* form with the same nature of the parent peak. These results clearly indicate the free rotation of 2,5-difluorobenzene in the macrocyclic cavity in both the *E* and *Z* forms.

To understand the chiroptical properties and racemization behavior of compounds **1** and **2**, CD spectroscopic studies of pure, separated enantiomers were carried out. The CD spectrum of (*E*)-**1**_A shows broad positive and negative bands at 307 and 433 nm, respectively, and the mirror image spectrum was observed in the case of (*E*)-**1**_B (Figure 5). After UV irradiation, (*E*)-**1**_A gave rise to a new CD spectrum with weaker positive bands at 300 and 324 nm, along with a more intense negative band at 416 nm; the mirror image spectra was observed for (*E*)-**1**_B. The reversal of the CD spectra to nearly the original state upon irradiation with visible light

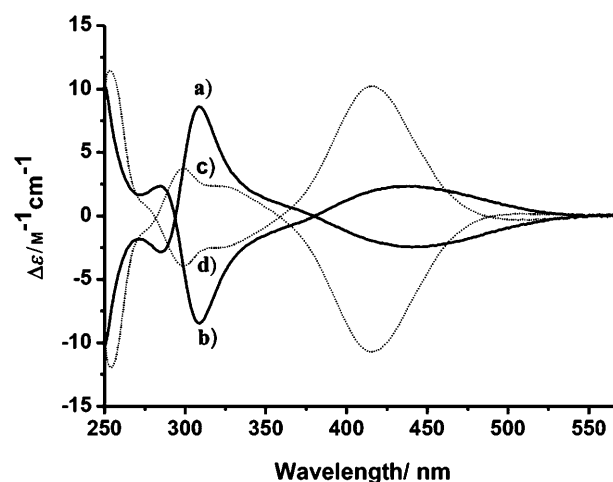


Figure 5. CD spectra of enantiomers of **1** in ethyl acetate; a) (*E*)-**1**_A, b) (*E*)-**1**_B, c) PSS_{366 nm} from (*E*)-**1**_A and d) PSS_{366 nm} from (*E*)-**1**_B.

clearly shows the absence of racemization in both the *E* and *Z* isomers of **1** (see the Supporting Information). Figure 6 shows the CD spectra recorded for the freshly separated

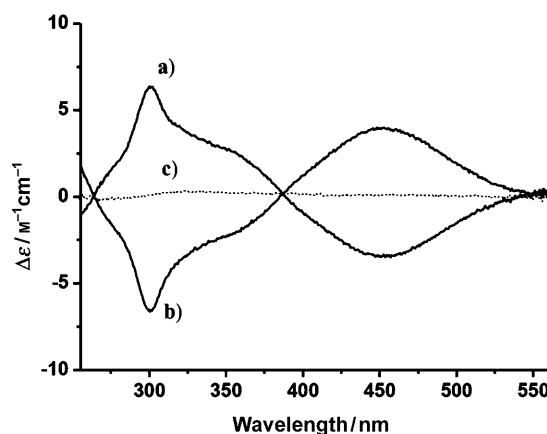
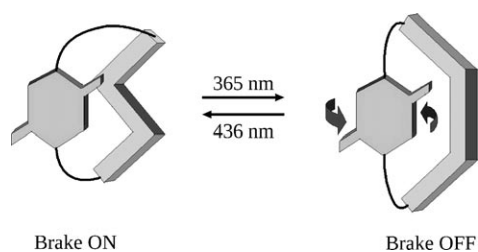


Figure 6. CD spectra of enantiomers of (*E*)-**2** in ethyl acetate; a) (*E*)-**2**_A, b) (*E*)-**2**_B and c) PSS_{366 nm} from (*E*)-**2**_A.

enantiomers of compound **2**. The CD spectrum of (*E*)-**2**_A (line a) shows broad positive and negative bands at 301 and 450 nm, respectively, and the complete mirror image spectrum (line b) was observed in the case of (*E*)-**2**_B. Interestingly, irradiation of (*E*)-**2**_A with light at 366 nm led to a gradual decrease in the CD signal, resulting in annihilation of the CD bands at the PSS (Figure 6). Irradiation of the resulting solution at 436 nm reversed the isomerization, keeping the CD signal silent. A similar observation was also made in the case of (*E*)-**2**_B. Thus, CD studies were also indicative of photoinduced racemization of the pure enantiomers due to *E/Z* isomerization upon irradiation with light at 366 nm. Nevertheless, at -10 °C the CD band did not disappear at the PSS upon UV irradiation; instead, a new CD band assignable to the *Z* isomer was formed. The intensity of this new CD band gradually decreased over 100 min in the dark at

–10°C (see Figure S11 in the Supporting Information). This indicates that rate of rotation of the 2,5-dimethylbenzene moiety is lowered at –10°C. From the results of the HPLC and CD experiments we are able to conclude that the rotor motion is controlled both by the bulkiness of the substituent on the rotor and by *E/Z* photoisomerization of the azobenzene moiety. Compound **1**, with methoxy substituents on the benzene rotor, represents the brake ON (rotation OFF) state in both the *E* and *Z* isomers, while **2**, with less bulky methyl substituents, is in the brake ON state in the *E* isomer and the brake OFF (rotation ON) state in the *Z* isomer (Scheme 3). Compound **3**, with fluorine substituents,



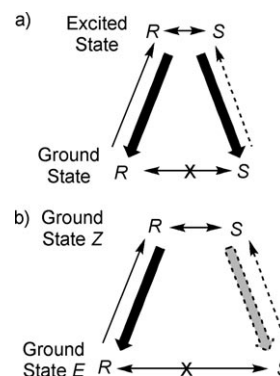
Scheme 3. Schematic representation of a photoinduced molecular brake.

is in the brake OFF state regardless of changes in cavity size as a result of photoisomerization. Compound **4** can also be expected to be in the brake OFF state in both the *E* and *Z* isomers, because the fluorine atom in compound **3** is replaced with smaller hydrogen atoms in **4**.

A study of the transition state of the rotational motion using space-filling molecular models gives further evidence for the brake action of compound **2**. Rotation of the benzene moiety in (*E*)-**2** is blocked by the aromatic part of the azobenzene, so the construction of an acceptable model for the transition state is impossible. In (*Z*)-**2**, the rotor part is accommodated within the macrocycle cavity in the transition state. Due to the small size of the fluorine atom in compound **3**, the rotor part is accommodated within the macrocycle cavity in the transition state even for the *E* isomer, which allows clear rotation in both the *E* and *Z* isomers (see Figure S14, in the Supporting Information). In comparison with our previous design, for which we demonstrated a complete ON/OFF switching by tuning the macrocyclic cavity size with different methylene spacers, here we achieved a similar ON/OFF switching of the benzene rotor by tuning the size of the rotor within the macrocyclic cavity with methylene spacers of fixed length.

Photoresolution by circular polarized light: The main objective of our study was to examine the possibility of chiral induction of racemic **2** by exposure to CPL. Among the various monocyclic azobenzenes synthesized, compound **2** was found to be most suitable for a photoresolution process in which irradiation of a racemate with *r*- or *l*-CPL will cause a partial enrichment of one of the enantiomers. Several compounds have been reported to undergo CPL photoresolution

through a chiral discrimination path from the electronic ground states to a common excited state^[18,27] (Scheme 4a). However, in the case of compound **2**, we propose a new



Scheme 4. Photochemical reaction with chiral induction by CPL irradiation. a) Reference [18,28] with an excited state for racemization; b) Compound **2** with a ground state *Z* isomer for racemization.

chiral discrimination path involving enantio-differentiating photoisomerization between the ground states of *R* and *S* enantiomers of *E* (E_R and E_S) and a common (or fast racemizing) ground state of the *Z* form (Scheme 4b). Thus, when a racemic mixture is irradiated with nonpolarized light, both *R*-to-*R* (solid line) and *S*-to-*S* (dotted line) *E/Z* isomerization pathways have the same efficiency, whereas upon CPL irradiation, one of the enantiomers may interact preferentially with *r*- or *l*-CPL, causing an enantiomeric imbalance to develop during repeated isomerization with the reverse *Z/E* isomerization path (thick line) (Scheme 4b).

Compound **2** possessed properties that were suitable for a chiral induction study by CPL; there was no racemization in *E* isomer and fast racemization in *Z* isomer in the electronic ground state at room temperature, and photoisomerization from *E* to *Z* and vice versa took place to reach the *E*-enriched PSS at 488 nm with a large $\Delta\epsilon$ at the same wavelength. The racemate (*R,S*)-(*E*)-**2**, upon CPL irradiation at 488 nm for 15 min resulted in enrichment of one of the enantiomers as evidenced by the change in the CD spectrum from inert to active. Further irradiation with CPL at the same wavelength with *l*- and *r*-CPL, induced an active CD that switched between positive and negative signs at the $n-\pi^*$ transition band (Figure 6).

Because the peak shape and position of the induced CD spectrum at the monitored wavelength for the solution irradiated with CPL matched those of one of the pure enantiomers of (*E*)-**2**, we were satisfied that one of the enantiomers was partially enriched. Further irradiation with nonpolarized light resulted in a silent CD spectrum, that is, the compound returned to a racemic state. This modulation was entirely reproducible in independent experiments and no deterioration of the modulated CD signal was seen during eight cycles (Figure 7, inset)

The maximum enantiomeric excess (*ee*) under *l*-CPL was obtained by using Equation (1); it is assumed that the molar

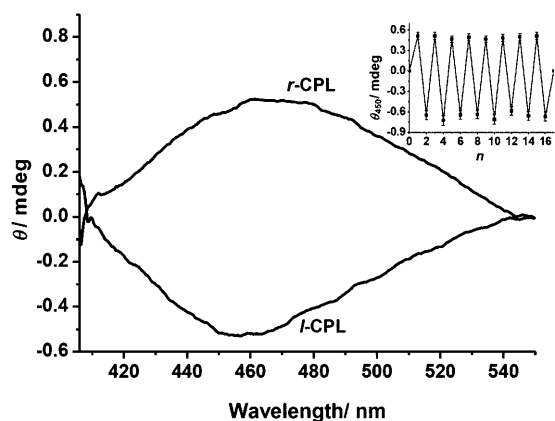


Figure 7. CD spectrum of **2** in ethyl acetate upon irradiation with *r*- and *l*-CPL at 488 nm. The difference in the CD absorption at 450 nm for a solution of **2** upon alternating irradiation with *r*- and *l*-CPL and nonpolarized light ($n=0-16$) with error bars estimated by a standard error of mean values of independent experiments (inset).

extinction coefficient of the *S*-*E* isomer was larger than that of the *R*-*E* and the *S*-*Z* isomer was larger than the *R*-*Z* isomer for *l*-CPL (see the Supporting Information for detailed calculations).

$$\frac{[R-E] - [S-E]}{[R-E] + [S-E]} = \frac{2\varepsilon_Z\Delta\varepsilon_E - 2\varepsilon_E\Delta\varepsilon_Z}{4\varepsilon_E\varepsilon_Z - \Delta\varepsilon_E\Delta\varepsilon_Z} \quad (1)$$

Experimentally obtained values of 125, 207, 1.72 and 1.44 L mol⁻¹ cm⁻¹ for ε_E , ε_Z , $\Delta\varepsilon_E$, and $\Delta\varepsilon_Z$ at 488 nm, respectively, were substituted into the equation to calculate the maximum enantiomeric excess under *l*-CPL irradiation [Eq. (2)].^[29]

$$\frac{[R-E] - [S-E]}{[R-E] + [S-E]} \times 100 = 0.34\% \quad (2)$$

By using the experimentally obtained value of $\Delta\varepsilon_E$ at 450 nm for the pure enantiomer and the induced CD value of 0.57 mdeg at 450 nm for the 2.2 mM solution of racemic **2** at PSS_{488 nm}, we calculated the photoinduced *ee* of the *E* isomer to be 0.30%, which is in reasonably good agreement with the theoretically estimated value.

In our previous bicyclic system, in which photoisomerization among the three isomers *EE*, *EZ* and *ZZ* produced a complex induced CD spectrum with contributions from not only the *EE* isomer but also from the *EZ* isomer, only an incomplete evaluation of *ee* was possible. In contrast, compound **2**, with its simple *E/Z* photoisomerization path, made it possible to clearly show the induction of molecular chirality in the *E* isomer, which was observed as an induced CD band with the corresponding spectral features of pure *E* enantiomers.

Conclusion

We have introduced a new class of light-driven molecular machines, based on macrocycles consisting of a 2,5-disubstituted-1,4-dioxybenzene rotating unit and a 3,3'-dioxyazobenzene photoisomerizable moiety bridged together by fixed bismethylene spacers. Among the different kinds of cyclic azobenzenes synthesized, compound **2**, with a 2,5-dimethylbenzene as rotor, was demonstrated to be a light-controlled molecular brake in which free rotation of rotor was completely stopped in the *E* isomer (brake ON, rotation OFF), whereas the rotation was allowed in the *Z* isomer (brake OFF, rotation ON). Compound **1**, with bulkier methoxy substituents at the 2,5-positions of the benzene rotor showed high conformational restriction of the free rotation of the rotor in both the *E* and *Z* isomers. Compound **3**, with a fluorine-substituted rotor, was observed to be in the brake OFF state, irrespective of changes to the cavity size as a result of photoisomerization. Thus, our design strategy showed that control of rotation of the benzene moiety can be achieved by appropriate functionalization on the benzene rotor as well as by photoisomerization of the azobenzene unit. More interestingly, cyclic azobenzene **2** has been successfully employed as a chiral sensor that can be used to show enantiomeric imbalance by detecting a chiral environment, such as CPL. Upon irradiation of racemate **2** with *r*- or *l*-CPL at 488 nm, we were able to repeatedly perform partial enrichment of the *S* or *R* enantiomers, respectively. We consider that this type of simple cyclic azobenzene constitutes a model that may be used to explain the asymmetric imbalance of molecules in nature through a new photoresolution path, that is, enantio-differentiation through photoisomerization between the ground states of stable *R* and *S* enantiomers of the *E* form and a rapidly racemizing ground state of the *Z* form.

Experimental Section

All solvents and chemicals were obtained from commercial sources and used without further purification, unless otherwise stated. NMR (¹H and ¹³C) spectra were recorded with a JEOL ECX 400 spectrometer using tetramethylsilane as an internal standard. Matrix-assisted laser desorption/ionization time-of-flight mass spectrometry (MALDI-TOF MS) was performed with an Applied Biosystems Voyager-DE pro instrument. X-ray crystallographic data were acquired with a Bruker Smart Apex diffractometer. Absorption spectra were recorded with an Agilent 8453 spectrophotometer. CD spectra were recorded with a JASCO J-S720 spectrophotometer. Photoisomerization studies were conducted using radiation from a super-high-pressure mercury lamp (500W, USHIO Inc.) after passage through appropriate filters (366 or 436 nm). High-pressure liquid chromatography (HPLC) was conducted with a Hitachi Elite La Chrome HPLC system using a CHIRALPAK IB (DAICEL Chemical Industries Ltd.) column to separate the enantiomers and analyze the *E/Z* and enantiomer ratio. Mixtures of ethyl acetate and hexane with ratios of 30:70 (for compound **1** and **3**) and 15:85 (for compound **2**) were used as eluent for the HPLC experiments. The *E/Z* isomer ratios at photostationary states were determined by NMR analysis or by HPLC monitored at a common isosbestic point, 273 nm.

General procedure for the synthesis of compounds 1, 2, and 4: A solution of dinitro compounds **5**, **6**, or **8** (2 mmol) in anhydrous THF (300 mL) was added dropwise over 6 h to a solution of LiAlH₄ (20 mmol) in anhydrous THF (100 mL) under an argon atmosphere. The reaction mixture was heated to reflux during the addition of the dinitro compound and was then stirred at RT for 12 h. After cooling the mixture in an ice bath, the reaction mixture was carefully quenched by the addition of water. The precipitate formed was filtered off and the solvent was evaporated under reduced pressure. The residual orange solid was redissolved in ethyl acetate or dichloromethane, and this solution was washed with water, brine, and dried over anhydrous MgSO₄. The solvent was removed under reduced pressure and the product was purified by column chromatography on silica gel to afford the desired product.

Compound (E)-1: Yield: 4.2% yield; orange solid; ¹H NMR (400 MHz, CDCl₃, 25 °C, TMS): δ = 7.48 (d, *J* = 6.8 Hz, 2H), 7.37 (dd, *J* = 8.0, 8.0 Hz, 2H), 7.13 (d, *J* = 4.2 Hz, 2H), 7.05 (d, *J* = 8.1 Hz, 2H), 6.7 (s, 2H), 4.62 (m, 2H), 4.37–4.52 (m, 6H), 3.69 ppm (s, 6H); ¹³C NMR (400 MHz, CDCl₃, 25 °C, TMS): δ = 159.0, 153.3, 144.7, 142.6, 130.1, 121.1, 115.1, 107.8, 104.5, 68.1, 65.3, 57.0 ppm; MS (MALDI-TOF): *m/z* calcd for C₂₄H₂₄N₂O₆: 437.16 [*M*+H]⁺; found: 437.89.

Compound (E)-2: Yield: 3.3%; orange solid; ¹H NMR (400 MHz, CDCl₃, 25 °C, TMS): δ = 7.47 (d, *J* = 7.9 Hz, 2H), 7.36 (dd, *J* = 7.9, 7.9 Hz, 2H), 7.03–7.05 (d, *J* = 8.6 Hz, 4H), 6.73 (s, 2H), 4.65 (m, 4H), 4.39–4.44 (m, 4H), 4.32 (m, 2H), 2.01 ppm (s, 6H); ¹³C NMR (400 MHz, CDCl₃, 25 °C, TMS): δ = 159.1, 153.2, 150.2, 130.0, 126.4, 120.9, 116.2, 115.5, 107.8, 67.0, 65.1, 16.4 ppm. MS (MALDI-TOF): *m/z* calcd for C₂₄H₂₄N₂O₄: 405.18 [*M*+H]⁺; found: 405.13.

Compound (E)-4: Yield: 3.5%; orange solid; ¹H NMR (400 MHz, CDCl₃, 25 °C, TMS): δ = 7.49 (d, *J* = 7.8 Hz, 2H), 7.36 (dd, *J* = 7.9, 7.9 Hz, 2H), 7.10–7.03 (m, 4H), 6.87 (s, 4H), 4.52 (t, *J* = 5.6 Hz, 4H), 4.49 ppm (t, *J* = 5.4 Hz, 4H); ¹³C NMR (400 MHz, CDCl₃, 25 °C, TMS): δ = 159.2, 153.7, 152.5, 130.0, 120.9, 117.0, 115.6, 108.5, 66.9, 65.2 ppm.

Synthesis of 3: Diisopropyl azodicarboxylate (DIAD; 1.62, 8 mmol) was added dropwise over 7 h to a mixture of 2,5-difluoro-1,4-hydroquinone (292 mg, 2 mmol), **7** (604 mg, 2 mmol) and triphenylphosphine (1.57 g, 6 mmol) in THF (300 mL) maintained at 0 °C under an argon atmosphere. The reaction mixture was slowly brought to RT and stirring was continued for 3 d. The solvent was evaporated and the residue was directly purified by chromatography over silica gel (ethyl acetate/hexane, 3:7) to obtain **3** as an orange solid (8 mg, 0.7% yield). ¹H NMR (400 MHz, CDCl₃, 25 °C, TMS): δ = 7.51 (d, *J* = 4.4 Hz, 2H), 7.39 (dd, *J* = 2.5, 7.9 Hz, 2H), 7.05 (m, 4H), 6.86 (dd, *J* = 9.8, 9.8 Hz, 2H), 4.51 (t, *J* = 5.9 Hz, 4H), 4.42 ppm (t, *J* = 5.7 Hz, 4H); ¹³C NMR (400 MHz, CDCl₃, 25 °C, TMS): δ = 158.7, 153.1, 144.1, 141.8, 137.1, 130.1, 121.1, 115.9, 107.9, 68.4, 65.1 ppm; MS (MALDI-TOF): *m/z* calcd for C₂₂H₁₈N₂O₄F₂: 413.12 [*M*+H]⁺; found: 413.10.

Compounds 5 and 6: A mixture of 2,5-dimethoxy or 2,5-dimethyl-1,4-dihydroxybenzene (10 mmol), and K₂CO₃ or NaH (22 mmol) in anhydrous DMF (20 mL) was stirred at RT for 1 h under an argon atmosphere. A solution of **9** (22 mmol) in anhydrous DMF (20 mL) was then added slowly and the mixture was heated to 60 °C for 12 h. After cooling to RT, the reaction mixture was added to an excess of water and the formed precipitate was washed with ethyl acetate and dried under vacuum overnight. The highly insoluble powder containing **5** or **6** was used for the next reaction without further purification.

Compound 5: Yield: 78.9%; pinkish powder; ¹H NMR (400 MHz, [D₆]DMSO, 25 °C, TMS): δ = 7.76 (d, *J* = 8.0 Hz, 2H), 7.72–7.70 (dd, *J* = 2.4, 2.4 Hz, 2H), 7.55 (dd, *J* = 8.2, 8.2 Hz, 2H), 7.44 (d, *J* = 8.1 Hz, 2H), 6.72 (s, 2H), 4.38 (t, *J* = 6.0 Hz, 4H), 4.26 (t, *J* = 5.3 Hz, 4H), 3.65 ppm (s, 6H); MS (MALDI-TOF): *m/z* calcd for C₂₄H₂₄N₂O₁₀: 501.15 [*M*+H]⁺; found: 501.79.

Compound 6: Yield: 30%; off-white powder; ¹H NMR (400 MHz, CDCl₃, 25 °C, TMS): δ = 7.86 (dd, *J* = 8.1 Hz, 2H), 7.83–7.79 (dd, *J* = 2.3, 2.3 Hz, 2H), 7.44 (dd, *J* = 8.2, 8.2 Hz, 2H), 7.30 (d, *J* = 8.3 Hz, 2H), 6.70 (s, 2H), 4.39 (t, *J* = 4.7 Hz, 4H), 4.30 (t, *J* = 4.7 Hz, 4H), 2.18 ppm (s, 6H); MS (MALDI-TOF): *m/z* calcd for C₂₄H₂₄N₂O₈: 469.16 [*M*+H]⁺; found: 469.97.

Compound 7: A mixture of 2-(3-nitrophenoxy)ethanol (1.83 g, 10 mmol), Zn powder (3.92 g, 60 mmol), and sodium hydroxide (2.4 g, 60 mmol) in ethanol/water (5:2, 70 mL) was heated to reflux for 20 min (disappearance of red color was observed). The reaction mixture was filtered and the filtrate was purged with air for 15 min. The filtrate was concentrated, extracted with ethyl acetate, washed with water, and dried over MgSO₄. The ethyl acetate was evaporated and the resulting orange solid was dissolved in hot methanol. Orange plate-like crystals of **7** were obtained (66% yield) by slow cooling of the solution. ¹H NMR (400 MHz, CD₃CN, 25 °C, TMS): δ = 7.34–7.30 (m, 6H), 7.25–6.90 (m, 2H), 3.92 (t, *J* = 4.8 Hz, 4H), 3.63 (t, *J* = 7.7 Hz, 4H), 2.81 ppm (t, *J* = 5.9 Hz, 2H); MS (MALDI-TOF): *m/z* calcd for C₈H₉NO₄: 303.13 [*M*+H]⁺; found: 303.19.

Compound 9: Diisopropyl azodicarboxylate (40% in toluene, 4.36 g, 21.57 mmol) was added dropwise to a mixture of 3-nitrophenol (2 g, 14.38 mmol), 2-bromoethanol (2.2 g, 17.27 mmol), and PPh₃ (5.66 g, 21.57 mmol) in THF (10 mL) at 0 °C under an argon atmosphere. After completion of the addition, the reaction mixture was allowed to slowly warm to RT and stirred overnight. Thereafter, the solvent was evaporated, the residue was extracted with CH₂Cl₂, and the combined extracts were dried over anhydrous MgSO₄. The product was purified by column chromatography on silica gel to obtain **9** (2.5 g, 71%) as a pale-yellow liquid. ¹H NMR (400 MHz, CDCl₃, 25 °C, TMS): δ = 7.24–7.87 (m, 4H), 4.38 (t, *J* = 5.7 Hz, 2H), 3.68 ppm (t, *J* = 5.7 Hz, 2H); ¹³C NMR (400 MHz, CDCl₃, 25 °C, TMS): δ = 158.7, 149.2, 130.3, 121.8, 116.4, 109.2, 68.5, 28.8 ppm; MS (MALDI-TOF): *m/z* calcd for C₈H₉BrNO₃: 245.97 [*M*+H]⁺; found: 245.28.

Induced circular dichroism by CPL irradiation: Prior to every measurement, the CD instrument was purged with nitrogen for at least 20 min and the temperature was set to 25.0 °C. The spectra were collected between 400–550 nm with a standard sensitivity of 100 mdeg, a data pitch of 0.5 nm, a bandwidth of 5 nm, a scanning speed of 20 nm s⁻¹ and a response of 2 s using a quartz cuvette (1 cm path length). Baseline correction and a binomial smoothing was applied to the induced spectral data. Samples were prepared in ethyl acetate solvent at a concentration of 2.2 mM and reference CD data were collected in the same solvent. The molecules obeyed the Beer–Lambert law at the monitored wavelength, suggesting that no molecular aggregation occurred at the given concentration (see the Supporting Information). Direct irradiation of the pure racemate with nonpolarized light using an Ar⁺ laser (488 nm) followed by irradiation through film filters (TCPR or TCPL of MeCan Imaging Inc. Japan) to produce *r*- or *l*-CPL at the same wavelength for about 15 min induced the CD signal. The filters were alternatively changed to produce *r*- or *l*-CPL to assess the reproducibility of the enrichment of the enantiomers.

Acknowledgements

This work was supported by a grant-in-aid for science research in a priority area “New Frontiers in Photochromism (No. 471)” from the Ministry of Education, Culture, Sports, Science, and Technology (MEXT), Japan. We thank Dr. Shin-ichiro Noro and Dr. Tsuyoshi Fukaminato, RIES, Hokkaido University for helping with the X-ray crystallographic analysis.

- [1] W. A. Bonner, *Top. Stereochem.* **1988**, *18*, 1–96.
- [2] A. S. Garay, *Nature* **1968**, *219*, 338–340.
- [3] K. Keosian, *The Origin of life*, 2nd ed., Reinhold, New York, **1968**.
- [4] S. Mason, *Chem. Soc. Rev.* **1988**, *17*, 347–359.
- [5] S. Kojo, *Symmetry* **2010**, *2*, 1022–1032.
- [6] I. Agranat, H. Caner, J. Cadwell, *Nature Rev. Drug Discov.* **2002**, *1*, 753–768.
- [7] a) S. K. Jha, K. S. Cheon, M. M. Green, J. V. Selinger, *J. Am. Chem. Soc.* **1999**, *121*, 1665–1673; b) K. Akagi, G. Piao, S. Kaneko, K. Sakamaki, H. Shirakawa, M. Kyotani, *Science* **1998**, *282*, 1683–1686; c) E. Yashima, K. Maeda, Y. Okamoto, *Nature* **1999**, *399*, 449–451.

- [8] a) Y. Furusho, T. Kimura, Y. Mizuno, T. Aida, *J. Am. Chem. Soc.* **1997**, *119*, 5267–5268; b) B. L. Feringa, R. A. van Delden, N. Koumura, E. M. Geertsema, *Chem. Rev.* **2000**, *100*, 1789–1816; c) S. Zahn, J. W. Canary, *Science* **2000**, *288*, 1404–1407.
- [9] D. K. Kondepudi, J. Laudadio, K. Asakura, *J. Am. Chem. Soc.* **1999**, *121*, 1448–1451.
- [10] B. Bosnich, *J. Am. Chem. Soc.* **1967**, *89*, 6143–6148.
- [11] H. Goto, Y. Furusho, E. Yashima, *Chem. Commun.* **2009**, 1650–1652.
- [12] a) B. L. Feringa, R. A. van Deldon, *Angew. Chem.* **1999**, *111*, 3624–3645; *Angew. Chem. Int. Ed.* **1999**, *38*, 3418–3438; b) S. F. Mason, *Nature* **1984**, *311*, 19–23; c) B. Norden, *Nature* **1977**, *266*, 567–568.
- [13] G. A. Hembury, V. V. Borovkov, Y. Inoue, *Chem. Rev.* **2008**, *108*, 1–73.
- [14] a) M. Mathews, N. Tamaoki, *J. Am. Chem. Soc.* **2008**, *130*, 11409–11416; b) N. Tamaoki, *Adv. Mater.* **2001**, *13*, 1135–1147; c) Y. Zhou, D. Zhang, L. Zhu, Z. Shuai, D. Zhu, *J. Org. Chem.* **2006**, *71*, 2123–2130; d) H. Akiyama, V. A. Mallia, N. Tamaoki, *Adv. Funct. Mater.* **2006**, *16*, 477–484; e) J. Ma, Y. Li, T. White, A. Urbas, Q. Li, *Chem. Commun.* **2010**, *46*, 3463–3465; f) Q. Li, L. Green, N. Venkataraman, I. Shiyankovskaya, A. Khan, A. Urbas, J. W. Doane, *J. Am. Chem. Soc.* **2007**, *129*, 12908–12909; g) T. J. White, R. L. Bricker, L. V. Natarajan, N. V. Tabiryan, L. Green, Q. Li, T. J. Bunning, *Adv. Funct. Mater.* **2009**, *19*, 3484–3488.
- [15] J. A. Le Bel, *Bull. Soc. Chim. Fr.* **1874**, *22*, 337–347.
- [16] J. H. Van't Hoff, *Die Lagerung der Atome im Raume*, 2nd ed., Vieweg, Braunschweig, **1894**.
- [17] M. Suarez, G. B. Schuster, *J. Am. Chem. Soc.* **1995**, *117*, 6732–6738.
- [18] a) N. P. M. Huck, W. F. Jager, B. de Lange, B. L. Feringa, *Science* **1996**, *273*, 1686–1688; b) *Molecular Switches* (Ed.: B. L. Feringa), Wiley-VCH, Weinheim, **2001**.
- [19] K. L. Stevenson, J. F. Verdick, *J. Am. Chem. Soc.* **1968**, *90*, 2974–2975.
- [20] a) C. Dugave, L. Demange, *Chem. Rev.* **2003**, *103*, 2475–2532; b) W. R. Browne, B. L. Feringa, *Nat. Nanotechnol.* **2006**, *1*, 25–35; c) T. Muraoka, K. Kinbara, Y. Kobayashi, T. Aida, *J. Am. Chem. Soc.* **2003**, *125*, 5612–5613; d) T. Muraoka, K. Kinbara, T. Aida, *Nature* **2006**, *440*, 512–515; e) V. Balzani, A. Credi, M. Venturi, *Chem. Soc. Rev.* **2009**, *38*, 1542–1550; f) M. Yamada, M. Kondo, J. Mamiya, Y. Yu, M. Kinoshita, C. J. Barrett, T. Ikeda, *Angew. Chem.* **2008**, *120*, 5064–5066; *Angew. Chem. Int. Ed.* **2008**, *47*, 4986–4988; g) K. Takaishi, M. Kawamoto, K. Tsubaki, T. Wada, *J. Org. Chem.* **2009**, *74*, 5723–5726; h) K. Nishizawa, S. Nagano, T. Seki, *J. Mater. Chem.* **2009**, *19*, 7191–7194.
- [21] a) J. L. Humphrey, M. L. Kimberly, M. E. Wright, D. Kuciauskas, *J. Phys. Chem. B* **2005**, *109*, 21496–21498; b) A. K. Flatt, S. M. Dirk, J. C. Henderson, D. E. Shen, J. Su, M. A. Reed, J. M. Tour, *Tetrahedron* **2003**, *59*, 8555–8570.
- [22] a) S. Yokoyama, M. Kakimoto, Y. Imai, *Thin Solid Films* **1994**, *242*, 183–186; b) A. Wu, M. Kakimoto, Y. Imai, *Molecular Crystals and Liquid Crystals* **1994**, *255*, 63–72; c) Z. F. Liu, K. Hashimoto, A. Fujishima, *Nature* **1990**, *347*, 658–660; d) S. L. Lim, N. J. Li, J. M. Lu, Q. D. Ling, C. X. Zhu, E. T. Kang, K. G. Neoh, *Appl. Mater. Interfaces* **2009**, *1*, 60–71.
- [23] a) J. M. Mativetsky, G. Pace, M. Elbing, M. A. Rampi, M. Mayor, P. Samorì, *J. Am. Chem. Soc.* **2008**, *130*, 9192–9193; b) B. Y. Choi, S. J. Kahng, S. Kim, H. Kim, H. W. Kim, Y. J. Song, Y. Kuk, *Phys. Rev. Lett.* **2006**, *96*, 156106; c) N. Katsonis, M. Lubomska, M. M. Pollard, B. L. Feringa, P. Rudolf, *Progress in Surface Science* **2007**, *82*, 407–434.
- [24] a) J. Barberá, L. Giorgini, F. Paris, E. Salatelli, R. M. Tejedor, L. Angiolini, *Chem. Eur. J.* **2008**, *14*, 11209–11221; b) G. Iftime, F. L. Labarthe, A. Natansohn, P. Rochon, *J. Am. Chem. Soc.* **2000**, *122*, 12646–12650.
- [25] N. Tamaoki, M. Wada, *J. Am. Chem. Soc.* **2006**, *128*, 6284–6285.
- [26] M. C. Basheer, Y. Oka, M. Mathews, N. Tamaoki, *Chem. Eur. J.* **2010**, *16*, 3489–3496.
- [27] a) M. H. Chang, B. B. Masek, D. A. Dougherty, *J. Am. Chem. Soc.* **1985**, *107*, 1124–1133; b) R. Ballardini, V. Balzani, J. Becher, A. D. Fabio, M. T. Gandolfi, G. Matternsteig, M. B. Nielsen, F. M. Raymo, S. J. Rowan, J. F. Stoddart, A. J. P. White, D. J. Williams, *J. Org. Chem.* **2000**, *65*, 4120–4126.
- [28] Y. Inoue, *Chem. Rev.* **1992**, *92*, 741–770.
- [29] The value of $\Delta\epsilon_z$ was obtained from the CD spectrum (Figure S11 in the Supporting Information) measured immediately after UV irradiation at 263 K.

Received: December 7, 2010

Published online: May 12, 2011